Proceedings of the 5th International Conference on Soft Computing for Security Applications (ICSCSA-2025)
DVD Part Number: CFP256A9-DVD; ISBN: 979-8-3315-9490-9

Enhanced Short-Term GHI Prediction Using Cloud-Aware Deep Autoencoder Network

1st Kalpalathika N
School of Computer Science Engineering,
Vellore Institute of Technology, Chennai
Tamil Nadu, India
kalpalathika.n2022@vitstudent.ac.in

2nd Jumin Salih
School of Computer Science Engineering,
Vellore Institute of Technology, Chennai
Tamil Nadu, India
jumin.salih2021@vitstudent.ac.in

3rd Lakshmi P
School of Computer Science Engineering,
Vellore Institute of Technology, Chennai
Tamil Nadu, India
lakshmi.2021@vitstudent.ac.in

4th Nihal Siddiqi
School of Computer Science Engineering,
Vellore Institute of Technology, Chennai
Tamil Nadu, India
nihal.siddiqi2021@vitstudent.ac.in

5th Bhuvaneswari A *
Assistant Professor,
School of Computer Science Engineering,
Vellore Institute of Technology, Chennai,
Tamil Nadu, India
bhuvaneswari.a@vit.ac.in

***Abstract*— Accurate short-term prediction of Global Horizontal Irradiance (GHI) is vital for reliable solar energy integration. This paper proposes a site-specific, data-driven forecasting framework combining clear-sky modeling with deep learning to capture cloud-induced variability. Visible-band satellite imagery is used to generate spatiotemporal cloud mask cubes, which are encoded via a Convolutional LSTM Autoencoder to learn cloud evolution patterns. These latent features, combined with clear-sky GHI estimates and temporal inputs, support multi-step forecasting. Cloud indices derived from normalized cloud masks help reconstruct ground truth GHI. Using a sliding-window approach, the model predicts four future steps from six past observations at 30-minute intervals. The proposed model is trained using a sliding-window approach, the model predicts four future steps from six past inputs. It achieves an R^2 value of 0.67, indicating good accuracy and the ability to learn meaningful patterns, making it suitable for operational solar nowcasting. The integration of cloud dynamics, radiative physics, and sequence learning yields accurate and interpretable GHI forecasts, suitable for operational nowcasting in data-limited settings. The resultant framework shows high potential for operational use in nowcasting systems, especially in data-scarce or satellite-only settings.**

Keywords—GHI, Solar Forecasting, Spatiotemporal Deep Learning, ConvLSTM, Satellite Imagery, PV, Cloud Prediction.

I. INTRODUCTION

With the global focus on renewable energy growing, solar power has come to be a key solution to achieving sustainable energy requirements. Despite this, the intermittency nature of solar radiation offers some constraints to grid integration, scheduling of energy, and system optimization. One key area of tackling these challenges is precise forecasting of Global Horizontal Irradiance (GHI)—total shortwave radiation per unit area on a horizontal plane—which is crucial in photovoltaic (PV) energy production, load dispatch planning, and ensuring energy reliability. Conventional approaches to GHI forecasting, including numerical weather prediction (NWP) models and ground sensor networks, typically face constraints such as coarse spatial resolution, delay, and low sensitivity to high-velocity changes in atmospheric conditions like cloud dynamics. Advances in recent years in high-resolution satellite imaging and machine learning have opened the door for a shift toward data-driven forecasting techniques. Deep learning algorithms with the ability to learn intricate spatial and temporal patterns offer a compelling solution to enhance forecasting accuracy.

The proposed research work develop a spatiotemporal deep learning architecture combining autoencoders and Convolutional Long Short Term Memory networks that are used to process visible channel satellite images and forecast GHI. Utilizing data from the INSAT series of geostationary satellites, the model learns the dynamics of cloud patterns and reconstructs image sequences, from which GHI values are computed via empirical cloud index calculations. The ability of the framework to provide accurate short-term predictions allows scalable deployment over different geographic areas independent of dense ground-based instrumentation. This demonstrates the revolutionary power of deep learning in closing the gap between meteorological measurements and solar energy prediction and making energy systems smarter and more responsive.

II. LITERATURE SURVEY

Accurate short-term forecasting of solar power is essential for the efficient operation of photovoltaic (PV) systems and maintaining grid stability. Traditional methods such as numerical weather prediction and optical flow-based cloud tracking often fall short when dealing with dynamic cloud formations and real-time application requirements. Consequently, satellite imagery combined with deep learning has emerged as a promising solution.

Several studies have explored advanced techniques to improve solar forecasting. One approach involves depth feature matching in satellite cloud images for enhanced motion estimation, which overcomes the limitations of gradient-based techniques [1]. Another method leverages temporal correlation

in satellite data to improve the accuracy of short-term PV forecasts [2]. To address the shortcomings of conventional machine learning models, attention-based deep neural networks have been proposed to help models prioritize significant cloud regions in input frames [3]. The direct use of satellite imagery, integrated with spatiotemporal modeling, has also demonstrated strong potential for reliable solar power forecasting [4].

The integration of data from multiple geostationary satellites, such as GEO-KOMSAT-2A and Himawari-8/9, has been shown to improve the accuracy of ground-level solar irradiance estimation [5]. Temporal forecasting has been further enhanced using hybrid models like LSTM–GANs, which successfully capture cloud motion dynamics over time [6]. Multi-layer cloud motion vector (CMV) forecasting techniques have also been introduced to account for vertical cloud structures, which are particularly relevant during complex atmospheric conditions [7]. The importance of near-real-time satellite updates has been emphasized in enhancing forecast responsiveness and reliability [8].

Operational implementations of satellite-based forecasting have revealed critical practical challenges, including spatial resolution and data latency, especially in real-world deployment scenarios [9]. Deep learning models have been suggested as robust alternatives to classical CMV approaches, leading to more stable and accurate irradiance forecasts [10]. Complementary research has focused on short-term prediction using raw satellite imagery [11], with early applications of machine learning involving Support Vector Machines (SVM) applied to satellite-derived features [12].

In the Indian context, studies utilizing Meteosat and INSAT-3D satellite data have underscored the need for regional calibration and model validation using ground-based measurements [13,14]. More recently, deep neural networks that incorporate spatiotemporal context have been found to significantly improve the accuracy of solar irradiance predictions [15]. This literature review highlights the transition from traditional forecasting techniques toward data-driven, deep learning-based models that are capable of leveraging satellite imagery for high-resolution, short-term solar power prediction.

III. Dataset Description

This paper introduces a spatiotemporal deep learning approach to short-term Global Horizontal Irradiance (GHI) forecasting using visible satellite images, cloud mask time series, and clear-sky irradiance simulation. It combines datadriven cloud recognition with physics-constrained irradiance prediction to forecast solar radiation for the next two hours every 30 minutes. The Indian National Satellite System (INSAT) series, developed and operated by the Indian Space Research Organisation (ISRO), consists of geostationary meteorological satellites such as INSAT-3D and INSAT-3DR. These satellites provide critical weather-related data through multi-spectral imagery in the visible, infrared (IR), and water vapor bands. With a temporal resolution of 15 to 30 minutes and spatial resolution as fine as 1 km, INSAT satellites are well-suited for near realtime monitoring of atmospheric phenomena. The satellite data is provided in Hierarchical Data Format version 5 (HDF5), which encapsulates multiple layers of spectral and derived atmospheric information. Among these, the visible band imagery is particularly significant for daytime monitoring of cloud coverage, movement, and intensity—key parameters that directly influence solar irradiance.

For this study, a dataset from the year 2019 was utilized, consisting of cloud imagery recorded at 30-minute intervals. Each HDF5 file contains several attributes such as IMG_VIS (Visible Band Reflectance), brightness, and cloud-top temperature. Throughout this project, the IMG_VIS attribute, representing visible band reflectance, was primarily used for the prediction of Global Horizontal Irradiance (GHI). A representative sample of the clipped image extracted from the INSAT-3D database is shown in Fig. 1, demonstrating the type of imagery used in this research.

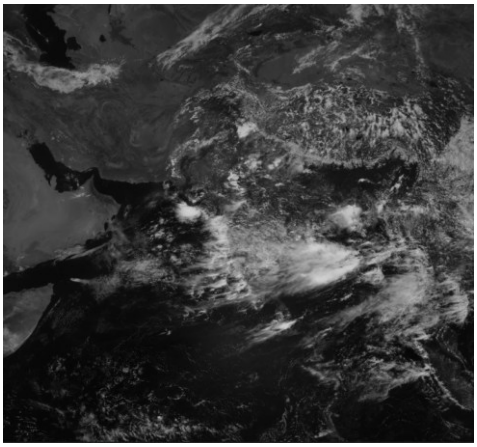

Fig. 1. Sample Visible Band Image from INSAT-3D Dataset (2019)

IV. Proposed Methodology

The following steps outline the complete pipeline (Fig. 2) for Global Horizontal Irradiance (GHI) forecasting using satellite cloud mask data and a ConvLSTM-based deep learning model. The overall proposed work pipeline is illustrated in Fig. III.2.

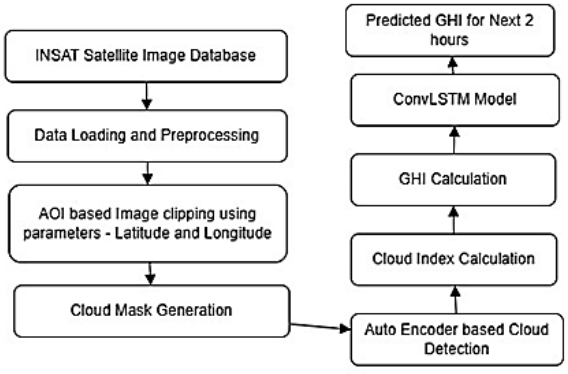

Fig. 2. Proposed GHI Pipeline

The pipeline starts with satellite images from the INSAT database, followed by AOI-based clipping using location

coordinates. A cloud mask is generated, and an autoencoder-based detection identifies cloud regions. This leads to cloud index calculation, which is used for GHI estimation. Then, data preprocessing and preparation is done for training a ConvLSTM model. Finally, a ConvLSTM model predicts GHI for the next 2 hours, aiding short-term solar forecasting.

A. Data Acquisition

We begin by defining the Area of Interest (AOI) using geographic coordinates and altitude, generating a 1-minute resolution DatetimeIndex between the specified start and end times, and computing the theoretical clear-sky Global Horizontal Irradiance (GHI) using PVLib's simplified Solis model.

B. Cloud Mask Processing

Cloud mask data is loaded from .npy files, with each filename containing a timestamp that is extracted to build a chronological series. For each image, the mean cloud coverage value is computed by averaging the binary mask. All cloud masks and their respective mean values are then temporally aligned and stacked to ensure consistency with the GHI data.

C. Cloud Index Computation

To calculate the Cloud Index (CI), we first determine the 5th and 95th percentile thresholds of the mean cloud coverage values. The CI is then derived by scaling the mean cloud coverage between these percentile bounds. To mitigate noise and account for short-term variability, a 15-minute rolling average is applied and any resulting gaps are backfilled. Cloud Index is calculated using:

$$CI = 1 - \frac{N - N_{min}}{N_{max} - N_{min}} \quad (1)$$

Apply a 15-minute rolling average and backfill to smooth noise.

D. Actual GHI Estimation

For each valid timestamp in the dataset, the corresponding clear-sky Global Horizontal Irradiance (GHI) value is matched. The actual GHI is then computed using the formula:

$$GHI_{actual} = GHI_{clear} \times CI \quad (2)$$

where CI represents the Cloud Index. Any missing or invalid data points are filtered out to ensure the reliability of the resulting dataset.

E. Time Series Sequence

To model GHI forecasts, time-series sequences are constructed using a sliding window approach—six past observations (3 hours at 30-minute intervals) are used to predict four future steps (2 hours). The normalized data is split into training and validation sets and reshaped into 5D tensors to suit the ConvLSTM input format. The ConvLSTM architecture includes stacked ConvLSTM2D layers with batch normalization, followed by dense layers to output 4-step forecasts. The model is trained with the Huber loss and Adam optimizer, using callbacks like EarlyStopping, ReduceLROnPlateau, and ModelCheckpoint, with up to 150 epochs. Predictions are inverse-transformed to the original GHI scale and evaluated using MAE, RMSE, and R^2. Visualizations include actual vs. predicted GHI plots and loss curves to monitor model performance and convergence.

F. Satellite Imagery Data Preprocessing

Preprocessing satellite imagery (Fig. 3) is vital for improving GHI prediction accuracy using deep learning. We prepare the data for modeling, both the actual and clear-sky GHI values are normalized jointly using a MinMaxScaler. This transformation scales both arrays into the [0, 1] range, allowing the model to converge more efficiently during training and ensuring consistency between input features and prediction targets. Raw HDF5 satellite data containing multi-band, time-sequenced arrays were filtered to extract visible-spectrum images relevant to solar radiation and cloud patterns, maintaining temporal continuity. The images were then spatially clipped to the region of interest to reduce computational load and focus on local patterns. To handle intensity variations from atmospheric and seasonal effects, normalization (min-max scaling and z-score standardization) was applied, ensuring consistent inputs and enhancing model performance.

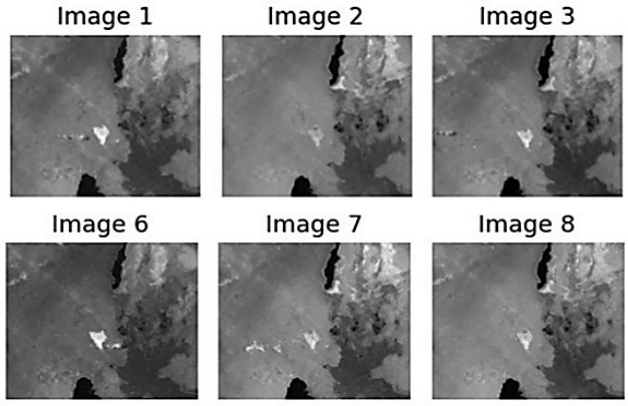

Fig. 3. Sequential satellite images of cloud movement.

G. Spatiotemporal Autoencoder Design

The proposed autoencoder architecture integrates both spatial and temporal modeling to forecast Global Horizontal Irradiance (GHI) using visible-channel satellite imagery. Input data (Table I) is structured as spatiotemporal cubes, capturing sequential satellite images that reflect cloud dynamics over time. The encoder leverages convolutional layers to extract spatial features, while temporal dependencies are modeled through Convolutional Long Short-Term Memory (ConvLSTM) layers. The decoder reconstructs future image frames, from which cloud indices are computed and subsequently used for GHI prediction.

TABLE I. INPUT AND OUTPUT DIMENSIONS OF THE MODEL

Stage	Description	Tensor shape
Input	Spatiotemporal cube	(6, 256, 256, 1)
Encoder Output	Compressed features	(6, 64, 64, 128)
ConvLSTM Output	Temporal representation	(64, 64, 128)
Decoder Output	Predicted next satellite frame	(256, 256, 1)

H. Cloud Detection and Masking

Cloud detection initiates GHI estimation by identifying cloud coverage through binary or probabilistic masks, which refine clear-sky GHI estimates without manual labeling. The Cloud mask and overlay visualization is shown in Fig. 4. A Cloud Index, computed from normalized mean pixel values and smoothed with a 15-minute rolling mean, quantifies cloud attenuation. Actual GHI is estimated as:

$$GHI(t) = CI(t) \times GHI\_clear - sky(t) \quad (3)$$

with clear-sky GHI from PVLib. An unsupervised autoencoder detects clouds via reconstruction error, where higher error indicates denser clouds. These adjusted GHI values are then used as inputs for ConvLSTM forecasting.

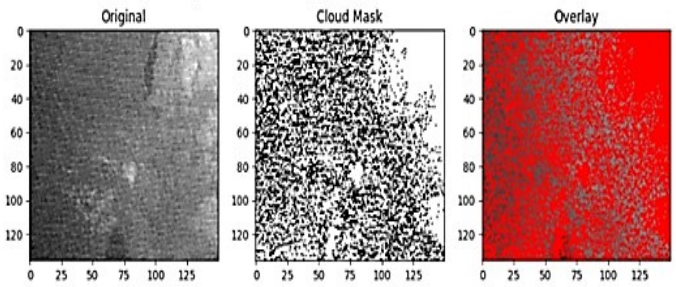

Fig. 4. Cloud mask and overlay visualization

Normalized cloud masks, based solely on visible reflectance, may struggle under haze, fog, or semi-transparent clouds due to low contrast. This can lead to inaccurate cloud index estimation and reduced GHI prediction accuracy. To improve performance, multi-spectral data (e.g., IR or SWIR) can be integrated for better cloud differentiation. Adaptive thresholding, meteorological data fusion, and post-correction can further refine cloud index accuracy under varying atmospheric conditions.

I. Temporal Modeling with ConvLSTM

ConvLSTM networks enhance GHI forecasting by capturing temporal dependencies in cloud motion from sequential satellite imagery. Using spatiotemporal image cubes as input, the model learns cloud dynamics while preserving spatial structure through its recurrent architecture. This enables accurate prediction of future irradiance, supporting solar energy applications such as resource planning, grid management, and short-term forecasting.

J. Autoencoder-Based Feature Learning

The proposed GHI prediction framework uses a spatiotemporal autoencoder to capture both spatial and temporal patterns in satellite imagery. The encoder extracts key features related to cloud movement and density, while ConvLSTM units model temporal evolution. The decoder reconstructs future frames to maintain temporal consistency, which are then used to compute cloud indices for GHI estimation. This data-driven approach efficiently handles satellite data complexities, offering a scalable and reliable solution for solar irradiance forecasting.

K. Model Layers and Hyper Parameters

The proposed spatiotemporal autoencoder for GHI prediction captures fine-grained spatial and temporal patterns in satellite data. The encoder uses convolutional layers with batch normalization and max-pooling to extract spatial features, while ConvLSTM layers preserve spatiotemporal dynamics of cloud behavior. The decoder reconstructs future image sequences using upsampling and transposed convolutions, ensuring motion continuity for accurate GHI estimation. Incorporating dropout and nonlinear activations, the model generalizes well across diverse weather conditions, enhancing the reliability of solar forecasting.

L. Training and Validation Protocol

The spatiotemporal autoencoder is trained to learn spatial and temporal patterns in satellite imagery for accurate GHI estimation. Using Mean Squared Error (MSE) loss, the model minimizes reconstruction errors in cloud textures and motion. The Adam optimizer ensures stable and efficient convergence, while mini-batch training and a learning rate scheduler enhance learning dynamics. Model checkpoints, early stopping, and loss monitoring prevent overfitting and support generalization. Data augmentation techniques like cropping and brightness adjustment improve robustness to varied cloud conditions, enabling reliable irradiance forecasting.

M. GHI Estimation from Reconstructed Frames

The last operation of the GHI forecasting pipeline consists of the estimation of Global Horizontal Irradiance (GHI) from reconstructed satellite image frames generated by the spatiotemporal autoencoder. One of the essential intermediary variables, the Cloud Index (CI), is derived from pixel-wise reconstructed frame brightness to indicate atmospheric transparency (0 when clear sky, 1 for complete cloud cover). By the use of CI maps, empirical radiative transfer models modulate clear-sky GHI values to indicate variations due to cloud.

$$\text{Actual GHI} = \text{Clear Sky GHI} \times \text{Cloud Index} \quad (4)$$

Post-processing normalizes and scales GHI values to be stable and compatible, rescaling outputs from 0 to 1 for analysis tasks

or remapping back into physical units (W/m²) for operational forecasting. This makes real-world application feasible within renewable energy systems, facilitating tasks such as photovoltaic plant optimization and grid management.

N. Model Optimization and Validation

The spatiotemporal autoencoder was trained to minimize prediction error, maintain stability under varying conditions, and generalize effectively. MSE loss tracked performance, while dropout (0.3–0.5), batch normalization, and L2 regularization helped prevent overfitting. Early stopping ensured the best model by halting training after validation loss plateaued. The ConvLSTM architecture was optimized, with a three-layer design balancing feature capture and computational efficiency. The Adam optimizer adjusted learning rates, and model checkpointing preserved weights. Sliding-window cross-validation confirmed the model's robustness and accuracy across seasonal changes, ensuring reliable GHI prediction for solar applications.

V. IMPLEMENTATION RESULTS AND DISCUSSION

A. Evaluation Metrics

To assess the precision and efficacy of the proposed cloud identification and GHI labeling model, three core metrics—Root Mean Square Error (RMSE), Mean Absolute Error (MAE), and Mean Squared Error (MSE)—are utilized. These metrics, commonly applied in regression analysis, are particularly significant for evaluating the model's ability to generalize solar irradiance estimations derived from satellite imagery based cloud masks. Their application ensures a reliable review of the model's predictive accuracy in estimating surface-level solar irradiance.

TABLE I. EVALUATION METRICS

Evaluation Metrics	Score
MAE (Mean Absolute Error)	128.81
RMSE (Root Mean Squared Error)	173.90
R^2 (R-squared)	0.67

RMSE is particularly sensitive to large errors due to the squaring of differences, making it suitable for penalizing outliers is shown in Table II. In this project, RMSE quantifies the accuracy of predicted GHI values derived from satellite image-based cloud masks against ground truth measurements from the Tirupati. Lower RMSE values indicate closer alignment with actual GHI data, reflecting higher model accuracy.

$$RMSE = \sqrt{\frac{1}{n}\sum_{i=1}^{n}(y_i - y_i')^2} \quad (5)$$

RMSE penalizes larger errors more than MAE. A score of 173.90 indicates some larger prediction errors exist in the dataset. The presence of larger prediction deviations might be due to sudden cloud changes, edge cases, or noise in satellite input. In addition, MAE evaluates the average error in GHI predictions, reflecting the impact of cloud misclassifications or data misalignments. Lower MAE values indicate higher prediction accuracy and alignment with actual observations.

$$MAE = \frac{1}{n}\sum_{i=1}^{n}|y_i - y_i'| \quad (6)$$

Predicted GHI values deviate by about 128.81 W/m² from the actual values. For GHI data this is a moderate error. A lower MAE (closer to 0) would suggest highly accurate predictions. 128.81 suggests that the model performs decently. MSE evaluates the deviation in GHI predictions caused by inaccuracies in cloud mask generation or model learning.

$$MSE = \frac{1}{n}\sqrt{\sum_{i=1}^{n}(y_i - y_i')^2} \quad (7)$$

The score tells much variance in actual GHI can the model can explain. A score of 0.67 means 67 percent of the variation in GHI is captured by the model.

$$R^2 = 1 - \frac{\sum_{i=1}^{n}(y_i - y_i')^2}{\sum_{i=1}^{n}(y_i - \overline{y}_i)^2} \quad (8)$$

R^2 values range from 0 (no explanation of variance) to 1 (perfect explanation). An R^2 of 0.67 is good level of accuracy.

It shows the model is learning meaningful patterns. With more data diversity, feature enrichment, or advanced modeling, the score can be improved if needed.

B. Prediction Accuracy and Visualization

Beyond numerical metrics, the model's prediction accuracy is further validated using graphical comparisons (Figure. 5). These visualizations offer insights into the model's performance and highlight specific areas for improvement: The following Fig. 5 (a) and Fig. 5 (b) shows cloud mask values at two different timestamps.

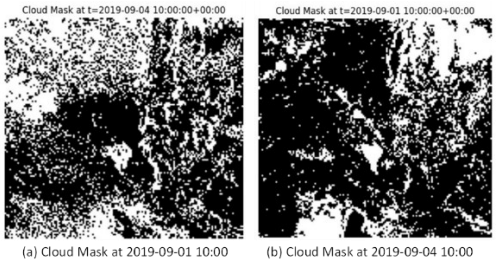

Fig. 5. Comparison of Cloud Masks at Two Different Timestamps

It can be further enhanced by integrating spatiotemporal cloud features through ConvLSTM layers, allowing the model to learn both spatial cloud structures and their temporal evolution across frames.

C. Actual Vs Predicted Graph

The comparative analysis (Table III) highlights the effectiveness of the prediction model in capturing spatial variability in solar irradiance across the region. The accuracy of spatial predictions for Global Horizontal Irradiance (GHI)

was assessed by comparing model outputs with ground truth data obtained from the Tirupati ground station.

TABLE II. GHI COMPARISON IN DIFFERENT TIMESTAMPS

Timestamp	Actual GHI (W/m²)	Predicted GHI (W/m²)
2019-09-01 11:00:00	730.6	654.8
2019-09-01 11:30:00	738.0	614.03
2019-09-01 12:00:00	753.8	687.9
2019-09-01 12:30:00	495.1	491.9

Fig. 6 shows the comparison of actual and predicted GHI at two different timestamps.

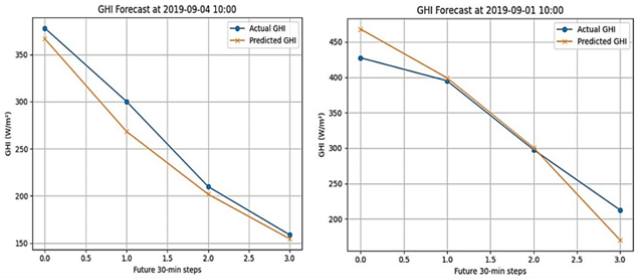

(a) GHI Forecast at 2019-09-01 10:00 (b) GHI Forecast at 2019-09-04 10:00

Fig. 6. Comparison of Actual and Predicted GHI at Two Different Timestamps

Heatmaps were employed to visualize irradiance intensity on a pixel-by-pixel basis, where lighter regions represent higher irradiance levels and darker regions indicate cloud coverage and reduced solar radiation. This method enables a visual evaluation of the spatial alignment between predicted and observed GHI, providing insight into the model's ability to replicate real-world solar radiation patterns. A graphical comparison of actual versus clear-sky Global Horizontal Irradiance (GHI) is illustrated in Fig. 7, which presents the superposition of actual, predicted, and ground truth GHI values.

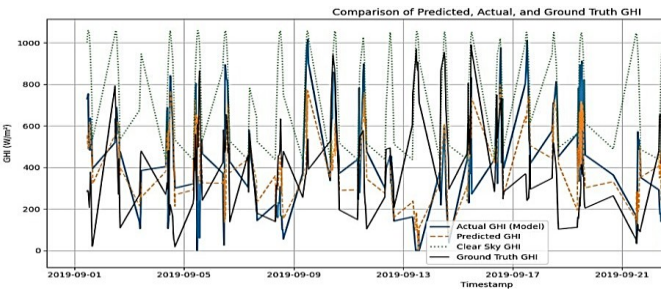

Fig. 7. Superposition of Actual vs Predicted GHI and ground truth values of GHI

To further evaluate the model's learning behavior, training and validation loss curves were analyzed. Ideally, the training loss decreases sharply and then stabilizes, while the validation loss follows a similar trend. A divergence between these curves—such as a continued decrease in training loss coupled with an increase in validation loss—indicates overfitting (Fig. 8). These loss curves were instrumental in selecting optimal model checkpoints and tuning key hyperparameters, including learning rate, batch size, and number of epochs. The presence of smooth and stable loss curves suggests effective learning dynamics, reinforcing the model's reliability in predicting solar irradiance.

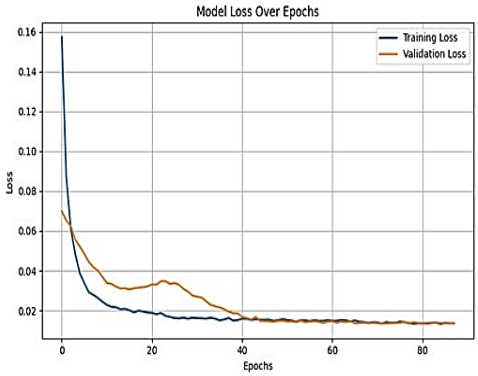

Fig. 8. Training and Validation Loss over Epochs

VI. CONCLUSION AND FUTURE WORK

This work presents a spatiotemporal deep learning framework that leverages an autoencoder-based ConvLSTM model to forecast Global Horizontal Irradiance (GHI) from visible-spectrum INSAT satellite imagery. By learning both spatial patterns and temporal cloud dynamics, the model effectively estimates surface-level irradiance, particularly in regions with limited ground-based sensor data. Efficiency is achieved by spatially clipping satellite imagery to a fixed Area of Interest (AOI), reducing computational overhead and enabling localized feature learning. {1.9} Preprocessing techniques such as regional clipping, cloud masking, and clear-sky GHI estimation via PVLib contribute to improved forecasting accuracy. The model, trained using MSE loss and the Adam optimizer, demonstrates stable convergence and effective cloud evolution tracking, making it suitable for operational short-term solar forecasting.

To further improve model performance, advanced preprocessing and training strategies should be employed, including Batch Normalization, Huber Loss, Dropout, and optimizers that ensure efficient convergence. Early stopping helps prevent overfitting, while region-specific fine-tuning and transfer learning enhance generalization and accuracy. In addition, the model's precision can be improved by enhancing cloud mask quality through multi-spectral data integration, refined thresholding, and post-processing techniques that reduce false detections and prediction variance.

ACKNOWLEDGMENT

The authors gratefully acknowledge the National Institute of Wind Energy (NIWE), Chennai, for their support and guidance in the development of this research. The expertise, resources, and insights provided by NIWE were instrumental in enhancing

the quality and relevance of this study on solar irradiance forecasting.

REFERENCES

[1] L. Zou, J. Wang, Y. Wang, and X. Liu, "A cloud motion estimation method based on cloud image depth feature matching," *IEEE Geosci. Remote Sensing Lett.*, vol. 22, pp. 1–5, 2025, doi: 10.1109/LGRS.2024.3491094.

[2] Y. Son, Y. Yoon, J. Cho, and S. Choi, "Cloud cover forecast based on correlation analysis on satellite images for short-term photovoltaic power forecasting," *Sustainability*, vol. 14, no. 8, p. 4427, Apr. 2022, doi: 10.3390/su14084427.

[3] M. Perera, J. D. Hoog, K. Bandara, and S. Halgamuge, "Distributed solar generation forecasting using attention-based deep neural networks for cloud movement prediction," *arXiv preprint*, arXiv:2411.10921, Nov. 2024, doi: 10.48550/arXiv.2411.10921.

[4] D. Yu, S. Lee, S. Lee, W. Choi, and L. Liu, "Forecasting photovoltaic power generation using satellite images," *Energies*, vol. 13, no. 24, p. 6603, Dec. 2020, doi: 10.3390/en13246603.

[5] C. K. Kim, H.-G. Kim, Y.-H. Kang, C.-Y. Yun, and Y. G. Lee, "Intercomparison of satellite-derived solar irradiance from the GEOKOMSAT-2A and HIMAWARI-8/9 satellites by the evaluation with ground observations," *Remote Sensing*, vol. 12, no. 13, p. 2149, Jul. 2020, doi: 10.3390/rs12132149.

[6] Y. Son, X. Zhang, Y. Yoon, J. Cho, and S. Choi, "LSTM–GAN based cloud movement prediction in satellite images for PV forecast," *J. Ambient Intell. Human Comput.*, vol. 14, no. 9, pp. 12373–12386, Sep. 2023, doi: 10.1007/s12652-022-04333-7.

[7] P. Kosmopoulos, A. Kazantzidis, A. M. S. Soulaymani, A. Retalis, and C. Cornaro, "Multi-layer cloud motion vector forecasting for solar energy applications," *Applied Energy*, vol. 353, p. 122144, Jan. 2024, doi: 10.1016/j.apenergy.2023.122144.

[8] A. A. Prasad and M. Kay, "Prediction of solar power using near-real time satellite data," *Energies*, vol. 14, no. 18, p. 5865, Sep. 2021, doi: 10.3390/en14185865.

[9] R. Alonso-Suarez, F. Marchesoni, L. Dovat, and A. Laguarda, "Satellite-based operational solar irradiance forecast for Uruguay's solar power plants," in *Proc. 2021 IEEE URUCON*, Montevideo, Uruguay, Nov. 2021, pp. 182–187. doi: 10.1109/URUCON53396.2021.9647087.

[10] N. Straub, S. Karalus, W. Herzberg, and E. Lorenz, "Satellite-based solar irradiance forecasting: Replacing cloud motion vectors by deep learning," *Solar RRL*, vol. 8, no. 24, p. 2400475, Dec. 2024, doi: 10.1002/solr.202400475.

[11] A. S. Devi, P. S. Kumar, R. G. Kumar, and T. M. Kumar, "Short-term solar power forecasting using satellite images," unpublished.

[12] H. S. Jang, J. W. Park, J. K. Park, and H. S. Kim, "Solar power prediction based on satellite images and support vector machine," *IEEE Trans. Sustain. Energy*, vol. 7, no. 3, pp. 1255–1263, Jul. 2016, doi: 10.1109/TSTE.2016.2535466.

[13] J. Polo, M. Sengupta, R. P. B. Santiago, and M. Pozo, "Solar radiation estimations over India using Meteosat satellite images," *Solar Energy*, vol. 85, no. 9, pp. 2395–2406, Sep. 2011, doi: 10.1016/j.solener.2011.07.004.

[14] H. G. Kamath and J. Srinivasan, "Validation of global irradiance derived from INSAT-3D over India," *Solar Energy*, vol. 202, pp. 45–54, May 2020, doi: 10.1016/j.solener.2020.03.084.

[15] O. Boussif, M. El Amine, A. Khacef, and A. Behloul, "Improving day-ahead solar irradiance time series forecasting by leveraging spatio-temporal context," presented at the *36th Conf. Neural Information Processing Systems (NeurIPS 2023)*, New Orleans, LA, USA, Dec. 2023. [Online]. Available: https://arxiv.org/abs/2306.01112.